USE OF A REACTION PATH MODEL TO IDENTIFY HYDROLOGIC STRUCTURE IN AN ALPINE CATCHMENT, COLORADO, USA

By

Jessica M. Driscoll

A Thesis Submitted to the Faculty of the

DEPARTMENT OF HYDROLOGY AND WATER RESOURCES

In Partial Fulfillment of the Requirements
For the Degree of

MASTER OF SCIENCE
WITH A MAJOR IN HYDROLOGY

In the Graduate College

THE UNIVERSITY OF ARIZONA

2009

STATEMENT BY AUTHOR

This thesis has been submitted in partial fulfillment of requirements for an advanced degree at The University of Arizona and is deposited in the University Library to be made available to borrowers under rules of the Library.

Brief quotations from this thesis are allowable without special permission, provided that accurate acknowledgement of source is made. Requests for permission for extended quotation from or reproduction of this manuscript in whole or in part may be granted by the copyright holder.

SIGNED: ____Jessica M. Driscoll_____

APPROVAL BY THESIS DIRECTOR

This thesis has been approved on the date shown below:

_____ _March 11, 2009_

Thomas Meixner
Associate Professor of Hydrology

Date

TABLE OF CONTENTS

ABSTRACT

Inverse geochemical modelling has been used frequently in groundwater systems between wells along a known flowpath and between precipitation and stream waters in catchments. This research expands the use of inverse geochemical modelling through a reaction path model (RPM) between waters in an alpine catchment to determine the geochemical connections and disconnections within the catchment. The data for this study are from the Green Lake 4 catchment in the Colorado Front Range during the 1996 snowmelt season, which has been divided into discrete time intervals based on snowmelt hydrology. Unique combinations of geochemical connections occur during these time intervals, and they show a dynamic hydrologic system. RPM results show notable disconnections; soil water is not geochemically connected to any other end member. These changes reflect changes in weathering reactions in the catchment that are dependent on the duration and timing of snowmelt. Previously end-member mixture analysis (EMMA) models have been used to discern the water sources in catchments over the last 20 years. Unification of the RPM and EMMA approaches offers the opportunity to connect the source of water to the internal hydrologic structure of the catchment, to better understand how catchments might respond to changes in climate or atmospheric deposition.

INTRODUCTION

The quantity and the quality of water resources in the western United States have been of increasing concern due to climate change impacts [Carroll and Cressie, 1996; Williams et al., 1996 Cline et al., 1998; Fassnacht et al., 2003]. Climate change threatens to alter the timing and duration of snowmelt in alpine catchments [Campbell et al., 1995; Stewart et al., 2004]. Snowmelt from alpine catchments provides 70-80% of water resources to the American Southwest [Doesken and Judson, 1997]. The lack of buffering capacity in these ecosystems makes them sensitive to changes in chemistry (e.g. acidic atmospheric deposition) [Hooper and Christopherson, 1992 ; Molotch et al., 2008; Williams et al., 1996].

Assessment of the hydrochemical impact of alteration of the timing and duration of snowmelt requires further understanding of the hydrologic structure at the catchment-scale [Hewlett, J.D. 1970; McGuire, 1973; Hooper, 2001; McDonnell, J.J., 2004]. The snowmelt-dominated hydrology of high elevation catchments drives chemical weathering reactions. Changes in these reactions can therefore indicate changes in hydrology within the catchment. Geochemical connections show likely hydrologic connections, and therefore changes in geochemical connectivity are linked to changes in hydrologic structure.

Our approach identifies hydrologic structure by finding the likely geochemical connections between hydrogeochemically distinct waters through mineral weathering reactions. The use of a reaction path model in this study identifies potential hydrologic flowpaths through the use of inverse geochemical reactions. These distinct source waters

are allowed to evolve during the snowmelt season to assess the changes in hydrologic structure over a seasonal timescale. Hydrologic structure is important to understand in order to forecast the impact of climate change on water quality in snowmelt-dominated catchments. There are several geochemical modeling approaches, however this study will focus on the Reaction Path Model (RPM).

Reaction Path Modelling Background

Reaction Path Modelling uses an inverse geochemical modelling approach [Garrels and Mackenzie, 1967; Mast and Drever, 1990]. A RPM uses a set of possible chemical reactions in the system to account for the geochemical difference between the two waters (Figure 2). More specifically, changes in composition must be explained by flux of solutes from weathered minerals and atmospheric input, and the flux of solutes from biomass and changes in the exchange pool [Drever and Clow, 1995]. A reaction path model uses the difference in geochemistry between two distinct catchment waters to determine the chemical reactions between the catchment waters. Generally this inverse geochemical approach is used for two groundwater wells along a known hydrologic gradient. This study expands the use of the RPM by applying a RPM to each combination of source waters in the catchment.

RPMs have several constraints. First, there are only certain minerals present and reactions possible. Physical stability of minerals constrain the reaction possibilities; the mineral stability series [Neese, 2000] describes the order in which minerals weather out of crystalline bedrock based on the stability fields of the minerals [Drever, 1988]. Primary minerals can dissolved at surface temperature and pressure, but cannot

precipitate at surface temperature and pressure. Secondary minerals can both dissolve and precipitate at standard temperature and pressure. The dissolution of minerals adds to solutes in solution, where as precipitation takes those solutes out of solution. These conditions are taken into account by disallowing the precipitation of minerals that were formed in higher temperature and pressure fields (e.g. hornblende) in the RPM.

RPMs allow the determination of the chemical connectivity of spatially distributed catchment waters. RPMs have been used to determine the suite of mineral weathering reactions between two waters along a given flowpath [e.g. Garrels and MacKenzie, 1967; Meixner et al., 1990; Mast and Drever, 1990; Williams et al., 1996; Bassett, 1997]. In this study each combination of catchment waters is tested to determine if the difference in chemical composition can be accounted for with a given set of mineral weathering reactions. A connection between these catchment waters is assumed when differences in hydrochemistry can be explained by the available mineral weathering reactions through precipitation or dissolution of available primary and secondary minerals in the catchment. In this study the biological component of this equation has been minimized by choosing an alpine watershed study site, where influence of biomass, and exchange pool changes are assumed to be negligible. Therefore the change in solute concentration between catchment waters can be accounted for by the difference in concentrations and incongruent mineral weathering.

The term “flowpaths” will be used often in this paper. We define “flowpath” to be a geochemical connection between two catchment waters that describes a potential hydrologic connection. Two catchment waters are deemed connected when the

difference in their composition can be explained by incongruent mineral weathering within the mineral assemblage and physical constraints of the catchment. Flowpaths between catchment waters are time independent; only the change in composition is used to determine a connection. Changes in these connections lead to conclusions about the hydrologic structure within the system.

Research Objectives

In this paper hydrochemical connections between distinct catchment waters are evidence for physical flowpaths. This approach will be used to address three research questions: (1) Can weathering reactions between catchment waters be estimated using an inverse geochemical model? (2) Are there hydrogeochemical connections between catchment waters in GLV and are these flowpaths persistent or intermittent in time? (3) Are there dominant flowpaths in each time period, and what do these flowpaths show about the nature and evolution of the hydrologic structure of the catchment? By addressing these questions, we hope to further understanding of the hydrology of alpine catchments with implications for identifying the impact of climate change on these ecosystems.

STUDY AREA

The Colorado Front Range is the eastern slope of the Continental Divide in the Rocky Mountains, which rise from the Colorado Plateau. The Green Lakes Valley (40° 03' N, 105° 35' W) an eastern-facing watershed of 700-hectacres. The Green Lake 4 watershed is located at the upper part of the Green Lakes Valley with an elevation range of 3250m to 4000m (Figure 2). The upper bound of the watershed at 4000m is the Continental Divide.

The underlying geology of the catchment is crystalline igneous bedrock, metamorphosed during the Laramide Orogeny in the late Cretaeous, approximately 80 to 35 million years ago (MYA). The bedrock is composed of sillimanite-biotite gneiss, granite, granodiorite, monzonite and monzogranite. There are two intrusions in the catchment: the Silver Plume and the Audubon-Albion. The Silver Plume quartz monzonite and monzogranite has U-Pb zircon age of 1400 MYA [Aleinikoff et al., 1990], and extends into the upper sections of the valley. The Audubon-Albion is a syenite with Rb-Sr age of 60-72 MYA, and is located only in the lower section of the GLV.

The northern bound of the GLV watershed is Niwot Ridge, where a metrological station and sampling have occurred in conjunction with the LTER Network and the Mountain Research Station since 1952. There is also a National Atmospheric Deposition Program (NADP) sample station on Niwot Ridge (NADP site ID = CO02). GLV is one of the catchments that supplies water to the City of Boulder.

GLV is made up of a series of stepped lakes, Lake Albion, Green Lake 1, Green Lake 2, Green Lake 3, Green Lake 4, Green Lake 5 and Arikaree Glacier (listed from

lower to higher elevation, respectively). These lakes are connected by seasonal wetland areas where surface water flows from lake to lake. The hydrology of the catchment is dominated by snowmelt, which occurs between May and October each year. Snowmelt contributes 80% of the total annual water input to the system [Caine, 1995].

The GL4 catchment spans an elevation of 3515m to 4000m at the Continental Divide. The GL4 catchment has an area of 225 hectares with a surface cover distribution of 29.6% rock, 33.6% talus, 30.1% soil, 2.8% glacier and 3.9% lake (Figure 4). GL4 is the most sampled watershed in the GLV, with weekly surface samples collected (when possible) since 1982.

METHODS

Sampling

This research uses the chemical and physical data collected during 1996 by the Niwot Ridge Long Term Ecological Research (LTER) site. The 1996 data were chosen in order to directly compare the results of this study with the results of the EMMA of Liu et al. [2004]. Samples were collected, as with Williams et al., [1996], of precipitation, snowpack, snow lysimeter, soil water, Arikaree glacier, Navajo meadow, talus water, rock glacier, GL5 and GL4.

All water and snow samples were analyzed for pH, acid neutralizing capacity (ANC), conductance, major ions (Ca, Mg, K, Na, Cl, SO_4, NO_3) and dissolved silica (Si) using protocols further described in Williams et al. [1996]. Snow samples were stored frozen at -20º C for 1-2 months until analysis. Snow samples were placed in covered polyethylene buckets and melted at room temperature. ANC was measured immediately after melting or on submission to the laboratory by Gran titration. Gran titration may underestimate ANC, particularly at low pH (<4.5) [Neal, 2001]. The pH in these waters is usually around 6 or 7 [Caine and Thurman, 1990], and therefore the underestimation is unlikely to be significant. Subsamples were immediately filtered through 47-mm Gelman A/E glass fiber filters with a 1-μm pore size. Filtered samples were stored in the dark at 4º C for subsequent analysis of major anions using a Dionex DX 500 ion chromatograph and cations using a Varian AA6 atomic absorption spectrophotometer within 1-4 weeks. Analytical error for all solutes was less than 2%, and the detection limit was less than 1

μeq L^{-1} [Williams and Caine, 2002]. End member chemistry values were obtained through personal communication with Niwot Ridge LTER researchers as well as the Niwot Ridge LTER online database [http://culter.colorado.edu/NWT/].

Catchment waters included in this study are precipitation (PP), snow pit (SP), snow lysimeter (SL), talus (EN1U, EN1M, EN1L, EN2U, EN2M, EN4U, EN4M, EN4V, averaged to be TLS), soil (SO), baseflow (BF), rock glacier (RG), Arikaree glacier (AK), Navajo Meadow (NV), Green Lake 5 (GL5) and Green Lake 4 (GL4). Sample locations are shown on the site map (Figure 2). The waters used were the same as the Liu et al. [2004] end members, with the addition of rock glacier data from 1998. Data from waters were converted to units of mmol/L, separated into time periods and then arithmetically averaged for that time period. The values for the entire year were also averaged into a summary for the year. The RG chemical data were separated into time periods based on the 1998 hydrograph. BF data were estimated to be the same as GL4 data at Julian day 66 (after Liu et al., 2004), when other inputs to GL4 are assumed to be minimal. This BF water composition is the closest sample to groundwater available.

Reaction Path Model

The inverse geochemical model used in this study required hydrochemical data of waters and precipitation and minerals present in the catchment. This study assumes that the chemical difference between distinct waters is attributed to the solute contribution from mineral weathering. Using a model to determine these mineral weathering reactions, we can find which waters may be connected by physical flowpaths, and the mineral weathering reactions dominant along that flowpath. Due to the short snowmelt

season and relatively small area of the catchment, the influence of evaporation on hydrochemistry is assumed to be small.

NETPATH [Plummer et al., 1991] was developed to use mass-balance equations between two groundwater wells to interpret the chemical evolution along a flowpath. PHREEQC, a chemical modeling program written by the USGS' Parkhurst [1995] later incorporated the mass-balance approach of NETPATH. Both NETPATH and PHREEQC perform mass-balance dissolution and precipitation reactions, however PHREEQC was chosen for this project because of the greater robustness of PHREEQC to determine uncertainties [Plummer and Appelo, 1991]. The greater robustness of the PHREEQC model lies in the greater number of equations PHREEQC uses in its calculations. In addition to mole-balance (which NETPATH also uses) PHREEQC uses charge-balance, electron-balance and alkalinity-balance equations [Parkhurst, 1997]. Within each of these balance equations PHREEQC allows for a user-defined amount of uncertainty, which increases the number of mineral weathering combinations.

The structure of PHREEQC allows the input of two water chemistries and the potential chemical reactions based on the mineral assemblage in the system. The details of these inputs are outlined in the next section. The parameters within PHREEQC were set to prevent physically impossible reactions and limited to only include combinations of mineral weathering reactions that would be within a 10% uncertainty of the measured compositional difference between the two catchment waters.

Model Inputs

The time period of the 1996 melt season was chosen as the focus of this study for the completeness of data, and to compare the results to the EMMA results of Liu et al. (2004). The hydrograph for the 1996 time period (Figure 3) was studied, and based on the shape of this hydrograph the snowmelt season was divided into three time periods (A, B and C). Period A starts at the beginning of snowmelt and lasts until the end of the initial snowmelt pulse (day of year (DOY) 148). Period B starts at this low point and continues to the peak of melt discharge (DOY 173). Period C starts at this peak and flow decreases as snowmelt drains from the catchment until temperatures decrease and water flow ceases (DOY 306).

Each chemical species measurement that was taken for the time period was averaged to determine a mean value for the time period for each water [Appendix A]. This approach not only allowed for an average composition for each water to be determined, but also made the quantity manageable. There was not data for each end member in every time period because of the progress of snowmelt.

Hydrochemical samples from each catchment water were input into the system as "solutions". The concentrations of ten chemical parameters (pH, ANC, Ca^{2+}, Si, Na^{+}, K^{+}, Mg^{2+}, SO_4^{2-}, Cl^{-} and NO_3^{-}) were input into the model for each of the waters. For each time period every combination of solutions was tested for geochemical connections. In other words, each water was used as the initial solution to every other water as the final solution.

In the water chemistry summary bar chart (Figure 4) the concentrations of each solute in each water are shown in a stacked bar chart. From these data it is clear that there is a high concentration of all solutes in the RG sample at all time periods, although magnified during Period C. Relative to the other time periods sampled, the concentrations of solutes for the SL and PP are higher during the initial pulse of snowmelt (Period A) then in any other time period. TLS water samples show generally low concentrations, though lowest during Period B, when the volume of liquid water is the highest in the catchment. The concentration of solutes increases after peak snowmelt, during Period C.

The suite of possible chemical reactions was determined by the characterization of geology to create the mineral assemblage. The geology of the catchment was chemically defined through sample collection based on geologic mapping and SEM analysis of samples [Platts-Mills and Williams, 2005] to determine the mineral assemblage for the GL4 catchment (Table 1). Primary minerals found in this analysis include plagioclase feldspar, potassium feldspar, hornblende and biotite. Pyrite was added to this assemblage based on personal communication with Williams and on-site observation. Secondary minerals (gibbsite, kaolinite, halite, smectite, goethite, calcite, gypsum) were added to this assemblage, generated as products of primary mineral weathering as well as eolian deposition. Each of these phases produces weathering products that can be added or subtracted to the waters of the catchment (Table 1).

Model Outputs

The RPM uses the available mineral assemblage to "explain" the hydrochemical difference between two waters. These explanation combinations are the output of the PHREEQC RPM. The explanations are not unique; there are multiple combinations of chemical reactions between each set of catchment waters [Appendix B]. Explanations are given in terms of mmol of phase change, where positive values indicate the phase has weathered and been added to the initial water chemistry, and negative values indicate that the phase has precipitated and solutes have been removed from the water.

Model Assumptions

The RPM, like any model, is not without assumptions. The following outlines the assumptions and their implications for the GL4 RPM:

- Accurate mineral assemblage includes all possible reactions. Alterations to this assemblage, or the reactions, will change the output of the model.
- End member chemistries adequately describe chemically discreet sources. The waters in this study were defined by Liu et al. [2004], and as comparison to EMMA was integral in this process, these waters remained the same.
- The average water concentrations for each time period accurately characterize the water. The values that are averaged are within a hydrologically-derived time period, and therefore the range of values is constrained within that time period. These values are therefore representative of the waters for that entire time period.
- The BF concentration accurately approximates the actual concentration of the water. It is unlikely that baseflow solute concentrations vary much during the snowmelt season, but this variable is unknowable because of the physical difficulty of measuring BF due to the terrain.
- Geochemical connections mean that there are physical hydrologic flowpaths between waters. Solute concentration can only increase through the reactions we have identified in the assemblage. It would be difficult to explain changes in concentration between two waters without a hydrologic connection.

These assumptions are mostly a reflection of the need to simplify a complicated system in order to run the RPM. The assumptions made with regard to the catchment waters in this study are inherited from the Liu et al. [2004] EMMA study.

RESULTS

Hydrochemistry

Chemical analyses of water samples show the variation in concentration of the same source water over the snowmelt season (Figure 4). The pH and ANC values are not plotted with the solutes because of the difference in unit measurement. The chemical data show a trend of a highly concentrated initial pulse (Period A), followed by a dilution to the peak of discharge (Period B) followed by a re-concentration of solutes as the volume of water in the catchment decreases (Period C). Also of note are the changes in proportion of solutes from one water to another. The RG water, for example, has a higher concentration of SO_4^{2-} and lower concentration of Cl^- than any other water. The lake waters (GL4 and GL5) are also more dilute than expected for their position on the hypothetical flowpath.

Reaction Path Modelling Results

The short and quick nature of flowpaths in this snowmelt-dominated catchment makes them difficult to physically observe. The chemically derived solution (RPM) allows for flowpaths to be determined geochemically in order to gain more insight on the hydrologic structure of the catchment. This RPM approach shows the amount of dissolution and precipitation of phases between two waters, however it does not incorporate the rate of weathering of the phases. As described in Section 2.2, the PHREEQC RPM provides chemical explanations for the difference between two water compositions. The results are non-unique because of the number of possible phases

allowing multiple solutions to the difference in chemistry. In an RPM, these chemical connections between waters can only be described by balanced weathering reactions (Table 1). Positive values mean the phase was added to the solution, either through weathering or in-gassing. Negative values mean the phase was removed from solution, either through precipitation or out-gassing. For each combination of waters that had an RPM result, there were multiple solutions. The multiplicity of solutions is the number of mineral weathering reaction combinations that could resolve the waters' hydrochemical difference. Most of these multiple solutions are very similar in total phase change values, and therefore average phase change for each flowpath could be used to evaluate the overall mineral weathering reactions along a given flowpath [Appendix B].

PHREEQC RPM Result Grid

Due to the multiplicity of results for each possible flowpath, a tabular system was developed in order to evaluate the PHREEQC results. Each combination of waters at both the initial and final point in the flowpath was attempted in PHREEQC for each time period. With eleven waters minus using the same solution as both the initial and final solution, there were 110 possible connections. This resulted in 110 possible solutions for each time period, plus the 1996 summary, 440 in total. The large number of non-unique results necessitated the creation of a method to visually display the results. Therefore an approach was created to view any overall trends of potential flowpaths during each time period. A grid was used to display each combination of one water to another, each grid space representing a different possible flowpath between two waters (Figure 5). The number of non-unique PHREEQC results is reported in this summarized format.

The eleven waters are listed at the top and along the side of each result grid. The waters are organized in an approximation of the hydrologic flowpaths assumed to exist, with the most dilute compositions (PP, SP) on the left and the most concentrated compositions (BF, RG, GL4) on the right. This order also generally corresponds to the highest to lowest elevation in the catchment. Each box represents the potential flowpath from the end member in the box directly above (initial water) it to the end member in the box to the left (final water). White boxes show no flowpath. Colored boxes show a geochemical connection, and the number inside the colored box shows the number of non-unique solutions possible for the difference in compositions. The light grey boxes show the flowpaths that cannot exist because there is no water sample during that time period. The dark grey boxes (diagonal) are in locations of flowpaths that would describe the same initial and final water.

The setup of the result grids allows for a visual analysis of the PHREEQC results for each time period, as well as a comparison between time periods. Because of the order of the waters, flowpaths that exist below the dark grey diagonal are physically assumed to exist. Flowpaths directly below the dark grey boxes are the most probable, as they are from one water to the next downgradient possibility. Flowpaths which are further from the diagonal are less expected and show connections that are not hydrologically intuitive (Figure 6).

Period A shows two flowpaths, from BF to GL4 and also from GL4 to BF. Period B shows fourteen flowpaths (AK to NV, GL5, TLS, BF and GL4; NV to GL5, TLS, BF and GL4; GL5 to BF, RG and GL4; TLS to BF; and GL4 to BF). Period C shows nine

flowpaths (AK to GL4; NV to GL5, TLS, BF, GL4; GL5 to BF, GL4; TLS to BF, GL4). The summary of the entire year shows fourteen flowpaths (AK to GL5, BF, GL4; NV to GL5, TLS, BF, GL4; GL5 to TLS, BF, GL4; TLS to GL5, BF, GL4 and GL4 to BF). These results show that waters are not consistantly connected via flowpaths for the entire snowmelt season (Figure 6).

The summary grid shows that there are patterns of flowpath connection within each period as well as between periods. In the summary grids vertical lines of flowpaths show that there is one initial water that is connected to several final waters. This water is a "source" of the flowpath. There are also horizontal lines in the summary grid, and these represent when several initial waters flow to the same final water. These final waters are "sinks" or reservoirs that receive flow from multiple locations.

The two dominant "sources" in the GL4 catchment are AK and NV. There are two "sinks", which are BF and GL4. The time period breakdown shows that the sinks are constant for all time periods, where as the sources vary between time periods.

DISCUSSION

The results show flowpaths between geochemically distinct waters within the catchment. The RPM results show definite disconnections (no geochemical reactions) and possible geochemical and therefore hydrological connections between waters. The ability to delineate the hydrologic structure in catchments, which will have an impact on the ability to more accurately model the hydrochemistry [Melack and Stoddard, 1991; Wolford et al., 1996; Meixner et al., 2000] as well as the physical hydrology [Clow and Mast, 2003; Williams et al., 2004].

Hydrologic Structure

Flowpaths are variable over time as not all geochemical connections exist for all three time periods. As shown in the summary grid, the RPM results in two flowpaths during Period A, fourteen during Period B and nine during Period C. The number of flowpaths in each period reflects the amount of hydrologic connectivity. The structure of this connectivity changes for each time period.

During Period A the only flowpaths are between baseflow and GL4, which is expected because most of the catchment waters were not sampled during this time period. The circular connection also makes sense because the source of the BF hydrochemistry is a water sample from GL4 before the start of snowmelt. The lack of other flowpaths during this period could be due to the short amount of time in this period as well as the lack of options due to cold temperatures during melt.

During Period B both AK and NV are connected to multiple downgradient waters (AK flows to five others, NV flows to four others). AK and NV are therefore defined as sources for flowpaths during this time period. There are also two dominant sinks, BF and GL4 that are the final water for five and three other waters, respectively.

Period C shows fewer flowpaths than Period B, with the notable exception of AK as a source as well as no connection to RG. This time period also has two dominant sinks, BF and GL4. There is no flowpath from GL4 to BF in this time period, which distinguishes it from Periods A and B.

The 1996 average grid shows fourteen flowpaths (same as Period B), however these flowpaths are different from the flowpaths shown in the time periods. There are some flowpaths that were seen in the time periods that are not seen in the summary (AK to NV, TLS; GL5 to RG) as well as some flowpaths that exist in this average that do not exist in the time periods (GL5 to TLS, TLS to GL5). These discrepancies show that flowpath change over the course of snowmelt, and using an average value for the entire season does not show those changes. The existence of flowpaths in the average summary that do not exist in the period summaries prove the importance of the time period segmentation based on hydrochemical concentrations and discharge.

The RPM allows the hydrochemistry of the source waters to vary over time by separating the snowmelt season into three time periods. This variation leads to an evolution of flowpaths during snowmelt, which indicates a change in hydrologic structure over time. The dominant sources of flowpaths in each period show a changing source of snowmelt and its varied connectivity to the hydrochemistry of the catchment.

In Period A, BF and GL4 are both the only sources of flow. In Period B, AK, NV and GL5 each have multiple connections. In Period C, NV, GL5 and TLS have multiple connections. The variability of geochemical connectivity in the catchment may reflect the variability of snowmelt flow in the catchment over the season.

The dependence of outflow in alpine catchments on baseflow has been noted in previous studies [Liu et al., 2004; Williams et al., 2004; Clow and Mast, 2003; Clow et al., 2003]. These studies were able to label baseflow as an important contributor to outflow, however the connection of baseflow to other source waters was not defined. The RPM shows not only the connection of baseflow to outflow, but also which waters contribute to baseflow recharge and how they change over time (GL4 in Period A, AK, NV, TLS, GL5 and GL4 in Period B and NV, GL5 and TLS in Period C). The ability to identify how these connections evolve during the snowmelt season will allow for comparison to the hydrochemical evolution during other years to assess the impact of changes of hydrochemistry as a result of climate change.

End Member Mixing Analysis vs. Reaction Path Model

End-member mixing analysis (EMMA) has been used to model the chemical contribution of catchment waters to a catchment output for the past 20 years. EMMA can be used to estimate the changing contribution of geochemically distinct catchment waters [Hooper and Chistopherson, 1990; Christopherson and Hooper 1992; Liu et al., 2004]. The driving principle of EMMA is that observed differences in outflow solute concentration are due to the variation in the contribution of hydrochemically static end member waters to the outflow over time.

EMMA does not allow catchment waters to interact, and therefore the intricacies of the chemical system are not well defined. Liu et al. [2004] found that there were three stages with different end member contributions during the 1996 snowmelt at GL4. The flowpaths in these stages were found using static end member compositions to calculate the contribution of those catchment waters to the GL4 output. Because of this, the EMMA model does not yield any information about end member contributions that do not influence the hydrochemistry of GL4, thereby missing critical hydrologic connections at the sub-catchment scale. RPM allows each end member to interact, focusing on the reactions to determine which catchment waters contribute to output composition.

The RPM was able to show geochemical connections between waters for each discrete time period during the 1996 snowmelt season. The RPM provided a suite of weathering reactions to explain the compositional difference between the two waters. Initial and final water combinations where no RPM solutions were found are assumed either to not be hydrologically connected or chemical processes other than mineral weathering were more dominant at that time.

RPM results not only show the possible geochemical connections between waters, but also the weathering reactions between these waters, which EMMA does not. Changes in geochemical connections also result in changes of mineral weathering reactions, which control the hydrochemistry of the output of the catchment. These reactions also provide the buffering capacity for alpine catchments. The RPM provides the ability to monitor the changes in weathering reactions within a snowmelt season and

between years will provide information on the hydrochemical impact of climate change to alpine catchments.

Evidence of Hydrologic Disconnection and Implications for the AHM

The influence of soils on stream water composition in alpine systems has been the driving question of several previous studies [Liator, 1987; Meixner et al., 2000]. The Alpine Hydrochemical Model (AHM) was developed to assess the hydrologic and biochemical responses in alpine catchments to changes in inputs of water, chemicals and energy. This model routs water through geochemical reaction boxes to determine the flux of solutes in the catchment. In this model the soil is included on a linear flowpath between talus and the lake output [Meixner et al. 2000]. Linking the RPM results with the AHM could help to improve these hydrologic assumptions.

There are no hydrochemical connections to or from the soil water samples in the RPM. These results suggest that the soil component of this model should be disconnected from the rock and talus components, altering the configuration of hydrologic flow and resulting geochemical reactions to have two separate geochemical systems intersecting at the outflow of the catchment. This hydrologic separation of the soil water from the rest of the system is an important distinction from other studies [Melack and Stoddard, 1991].

Evolution of hydrologic structure during the snowmelt season

The results of the RPM show the advantage of this hydrochemical model to gain understanding of the hydrologic processes within a catchment (Figure 7). The eleven

catchment waters are grouped into four categories; Upgradient Glacier (AK), Surface Waters (NV, GL5, GL4), Intermittent Waters (TLS, RG) and Baseflow Reservoir (BF). These categories were created with a hydrologic gradient in mind, with expected flow from the Upgradient Glacier to Surface Water to Intermittent Waters and Baseflow Reservoir. The difference in connectivity between these four categories is shown for each time period. Period A shows a connection between Surface Waters and Baseflow Reservoir, in both directions. Period B shows the Upgradient Glacier connected to each of the other three categories, and then connections from these categories to the expected downgradient category. Period C shows flow from the Upgradient Glacier to Surface Waters, and from Surface Waters to both Intermittent Waters and the Baseflow Reservoir.

These connections show the affect of a saturated catchment in Period B, returning to an expected flow pattern in Period C. Period B shows flowpaths that are physically more unrealistic (e.g. direct connection between the Upgradient Glacier and Baseflow Reservoir). These flowpaths between uppermost and lowest gradient waters are due to the combination of quickness of flow and homogeneous source water chemistry. These factors may be responsible for the lack of geochemical connections to intermediate waters. The further understanding of this hydrologic structure can be used to advance the use of the AHM through more accurate geochemical flow routing in the model.

CONCLUSIONS

This study used a RPM to define hydrologic structure within the GL4 catchment of Niwot Ridge. This RPM method used hydrochemical and geochemical data to produce information about the hydrologic flowpaths between waters that was used to define the hydrologic structure in the catchment. The RPM results show disconnections and possible connections between hydrochemically distinct catchment waters. A method to assess the probability of these possible connections still needs to be developed.

The disconnection of soil from the rest of the hydrologic system had been previously assumed, however this hydrochemical study has shown justification for this assumption. The separation of the soil subunits from the rest of the catchment may be due to a number of hydrobiogeochemical explanations, such as isolated reactions that occur over different residence time scales than the rest of the catchment.

The RPM showed that there were distinct geochemical connections between waters and that these connections varied over the course of snowmelt. The 1996 average chemical data showed a good fit for the overall flowpaths, but does not capture the variable hydrologic discontinuity over the course of snowmelt. There are three hydrologically defined time periods during the snowmelt season, and each have their own hydrologic structure. Period A is simple due to the lack of thawed source waters. Period B shows affects of excess saturation with geochemical connections between physically unrealistic waters. Period C shows a hydrologic structure along the assumed hydrologic gradient. This evolution of the hydrologic structure may be altered as the timing and

duration of snowmelt changes. This RPM method allows for evaluation of the affects of these snowmelt changes.

APPENDICES

A. TABLE

Phase	Chemical Formula	Weathering Reaction
K-Feldspar[1]	$KAlSi_3O_8$	$KAlSi_3O_8 + 8H_2O + CO_2 \Rightarrow Al(OH)_3 + 3H_4SiO_4 + K^+ + HCO_3^-$
Biotite[1]	$KMg_3AlSi_3O_{10}(OH)_2$	$KMg_3AlSi_3O_{10}(OH)_2 + 6H^+ + 4H_2O \Rightarrow K^+ + 3Mg^{+2} + Al(OH)_4^- + 3H_4SiO_4$
Plagioclase[1]	$Na_{0.62}Ca_{0.38}Al_{1.38}Si_{2.62}O_8$	$Na_{0.62}Ca_{0.38}Al_{1.38}Si_{2.62}O_8 + 5.52\ H^+ + 2.48H_2O \Rightarrow 0.62Na^+ + 0.38Ca^{+2} + 1.38Al^{+3} + 2.62H_4SiO_4$
Hornblende[1]	$Ca_{1.7}Na_{0.6}Mg_2Fe_2AlSi_7AlO_{22}(OH)_2$	$Ca_{1.7}Na_{0.6}Mg_2Fe_2AlSi_7AlO_{22}(OH)_2 + 22H_2O + 10CO_2 \Rightarrow 2Al(OH)_3 + 7H_4SiO_4 + 1.7Ca^{+2} + 0.6Na^+ + 2Mg^{+2} + 2Fe^{+2} + 2OH^- + 10HCO_3^-$
Pyrite[1]	FeS_2	$FeS_2 + 2H^+ + 2e^- \Rightarrow Fe^{+2} + 2HS^-$
Epidote[1]	$Ca_2Al_2FeOOHSiO_7$	$Ca_2Al_2FeOOHSiO_7 + 10H_2O + 3CO2 \Rightarrow 2Al(OH)_3 + H_4SiO_4 + 2Ca^{+2} + Fe^{+3} + 6OH^- + 3HCO_3^- + 2H^+$
Geothite[2]	FeOOH	$FeOOH + 3H^+ \Leftrightarrow Fe^{+3} + 2H_2O$
Kaolinite[2]	$Al_2Si_2O_5(OH)_4$	$Al_2Si_2O_5(OH)_4 + 5\ H_2O \Leftrightarrow 2Al(OH)_3 + 2H_4SiO_4$
Gibbsite[2]	$Al(OH)_3$	$Al(OH)_3 \Leftrightarrow Al^{+3} + 3OH^-$
Smectite[2]	$Ca_{0.17}Mg_{1.83}Al_2Si_2O_{10}(OH)_2$	$Ca_{0.17}Mg_{1.83}Al_2Si_2O_{10}(OH)_2 + 6H_2O + 4H^+ + 4e^- \Leftrightarrow 0.17Ca^{+2} + 1.83Mg^{+2} + 2Al(OH)_3 + 2H_4SiO_4 + 4OH^-$
Calcite[2]	$CaCO_3$	$CaCO_3 \Leftrightarrow CO_3^{-2} + Ca^{+2}$
Halite[2]	NaCl	$NaCl \Leftrightarrow Na^+ + Cl^-$
Carbon Dioxide[2]	CO_2	$CO_2 \Leftrightarrow CO_2$
DiNitrogen[2]	N_2	$N_2 + 6\ H_2O \Leftrightarrow 2\ NO_3^- + 12\ H^+ + 10\ e^-$

Table 1: Mineral assemblage and weathering products in GLV.
[1] primary mineral; [2] secondary mineral.

B. FIGURES

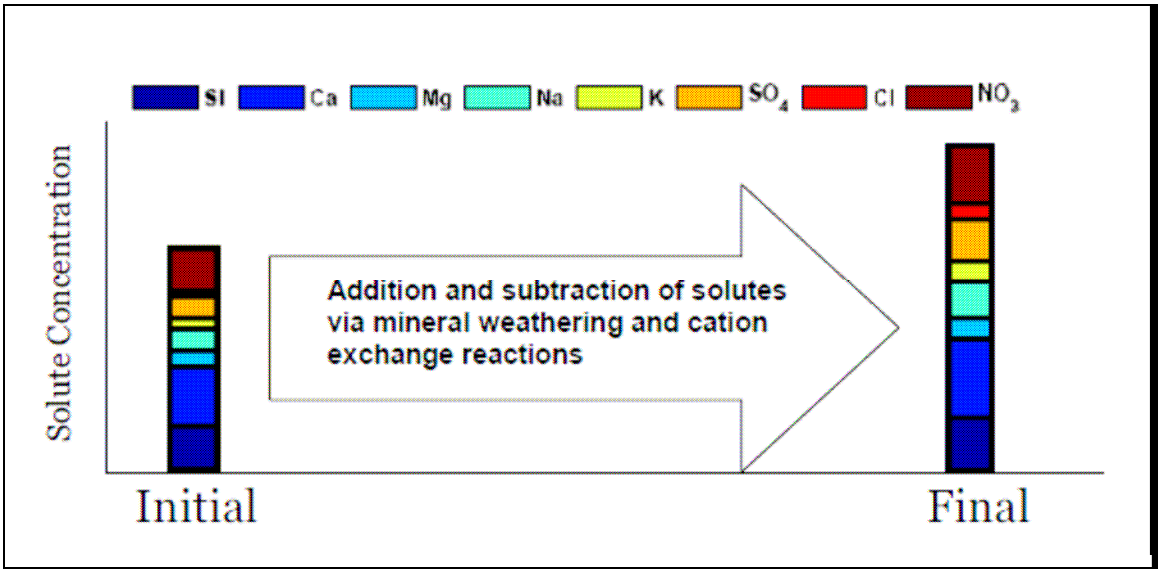

Figure 1: Reaction Path Modelling.
A RPM uses the concentrations of solutes in two waters (initial, left and final, right) and calculates the difference of those concentrations. If the difference in concentration could be caused by an addition or subtraction of solutes through possible geochemical reactions in the catchment then there is a possible hydrologic flowpath between the two waters.

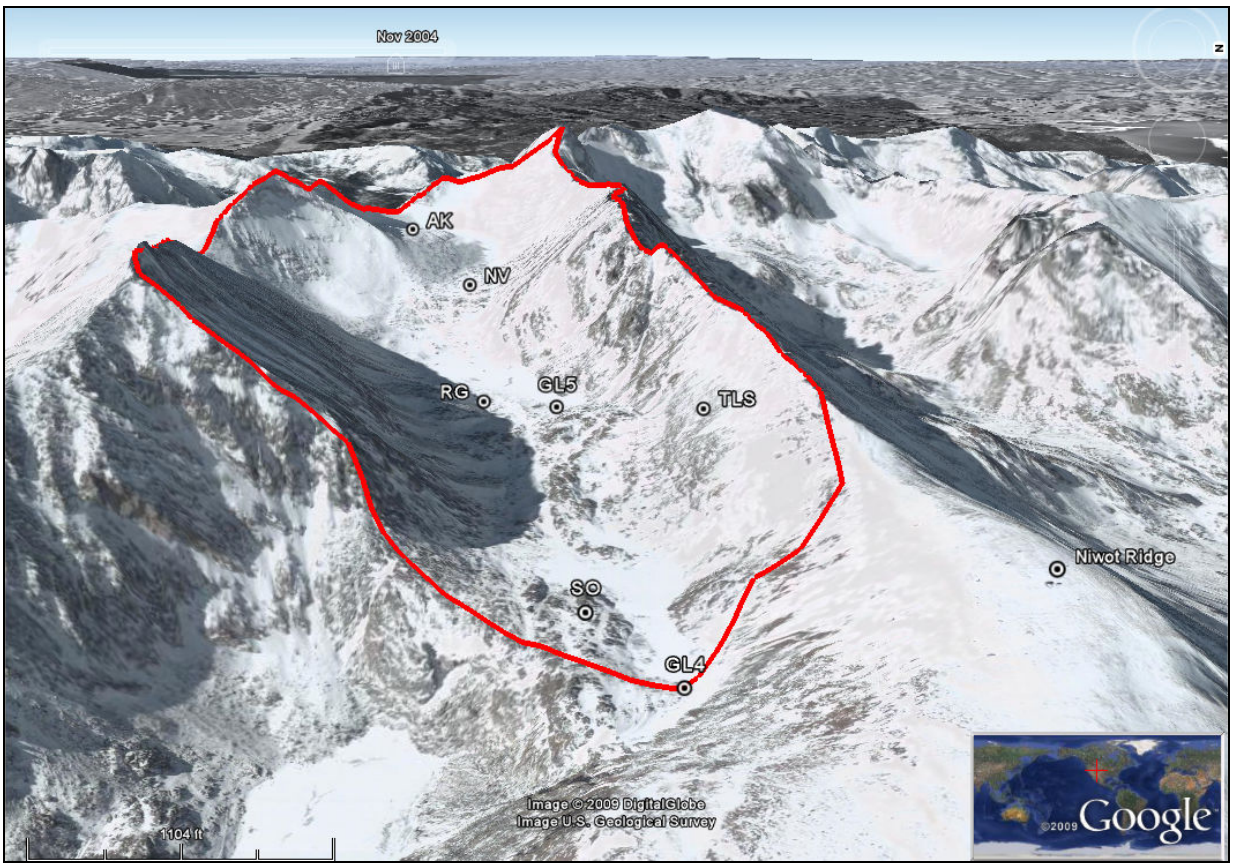

Figure 2: Site map of GL4 watershed.
The Green Lakes Valley is located on the eastern slope of the Colorado Rockies. The GL4 watershed is 225 ha and spans an elevation of 3250m to 4000m at the Continental Divide. The watershed is seen here in this GoogleEarth image from November 2004 facing west, with the watershed boundary outlined in red. Sample locations for each of the end member chemistries are shown with their abbreviations (AK- Arikaree Glacier, NV- Navajo Meadow, RG- Rock Glacier, GL5- Green Lake 5, TLS- Talus, SO- Soil, GL4- Green Lake 4). The marker labeled Niwot Ridge is the location of the research station where PP- Precipitation, SP- Snow Pit and SL- Snow Lysimeter samples were collected.

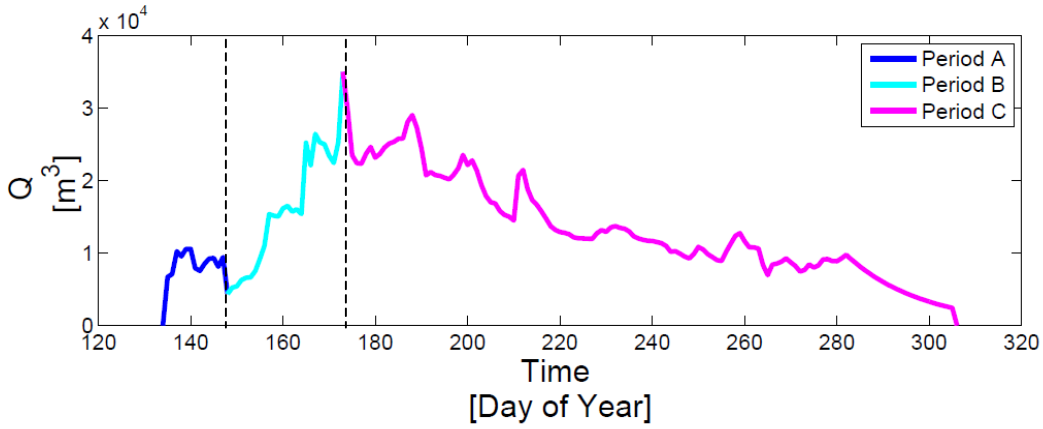

Figure 3: Hydrology of GL4.
The above figure shows the flow out of GL4 during the 1996 snowmelt season in Julian Days. The hydrograph shows a typical snowmelt pattern that has been divided into three time periods. Period A spans the initial snowmelt pulse. Period B starts at the beginning of the rising limb of the hydrograph and ends at the peak discharge. Period C starts at peak discharge and lasts until the end of the snowmelt season.

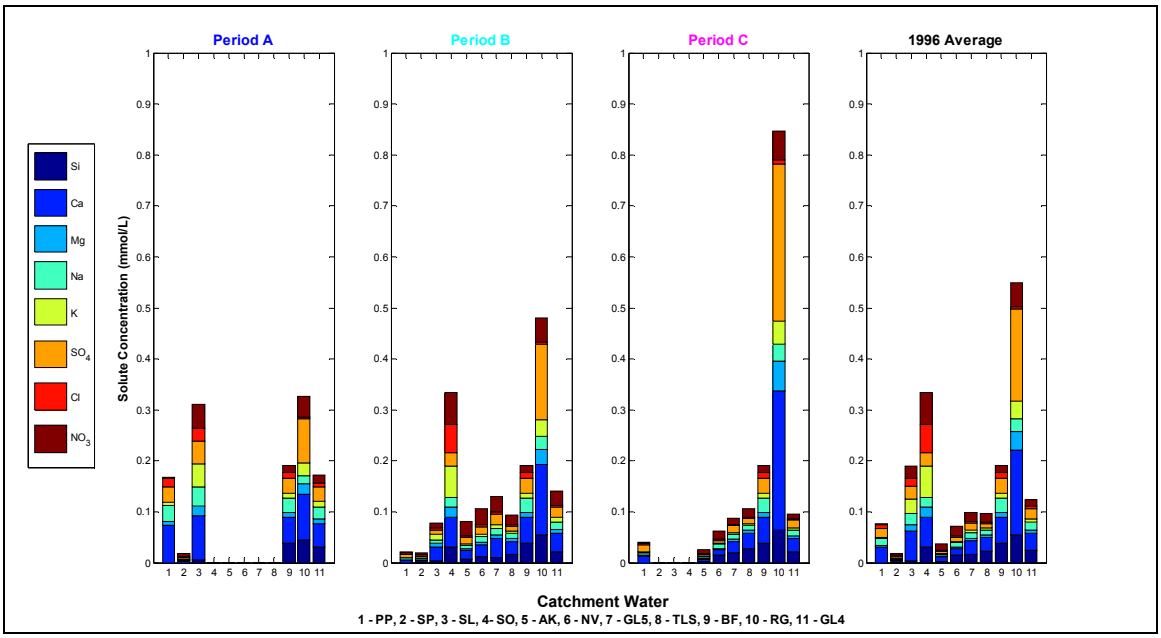

Figure 4: Concentrations of solutes for each water.
The above bar charts show the concentration of solutes (color chart seen below) for each of the defined time periods as well as the average values for the entire snowmelt season. The catchment waters are organized along the bottom of each chart in order of assumed hydrologic gradient, from PP to GL4. These charts show that the distribution of concentrations varies from water to water within the same time period as well as from time period to time period. It is this variability, the change in concentrations, which will be modeled using the RPM.

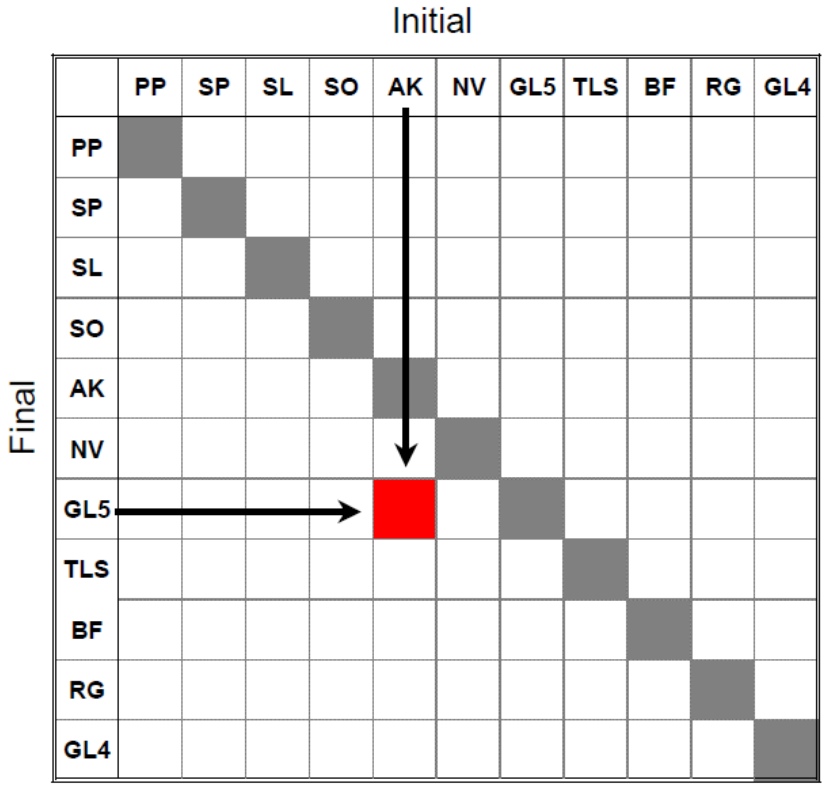

Figure 5: RPM Result Grid.
The results of the RPM were complicated to present, and therefore the above result grid was created. In each grid the initial waters are shown across the top (in the same hydrologic gradient order as previously explained) and the final waters are located down the side. This grid shows each possible combination of the eleven catchment waters in both initial and final pairings. The dark grey boxes are where the initial and final catchment waters are the same. In this example the red box shows a possible hydrologic connection from AK to GL5. It is important to note that the colored boxes in these grids show where connections are possible based on the geochemistry, they do not prove that a physical flowpath exists.

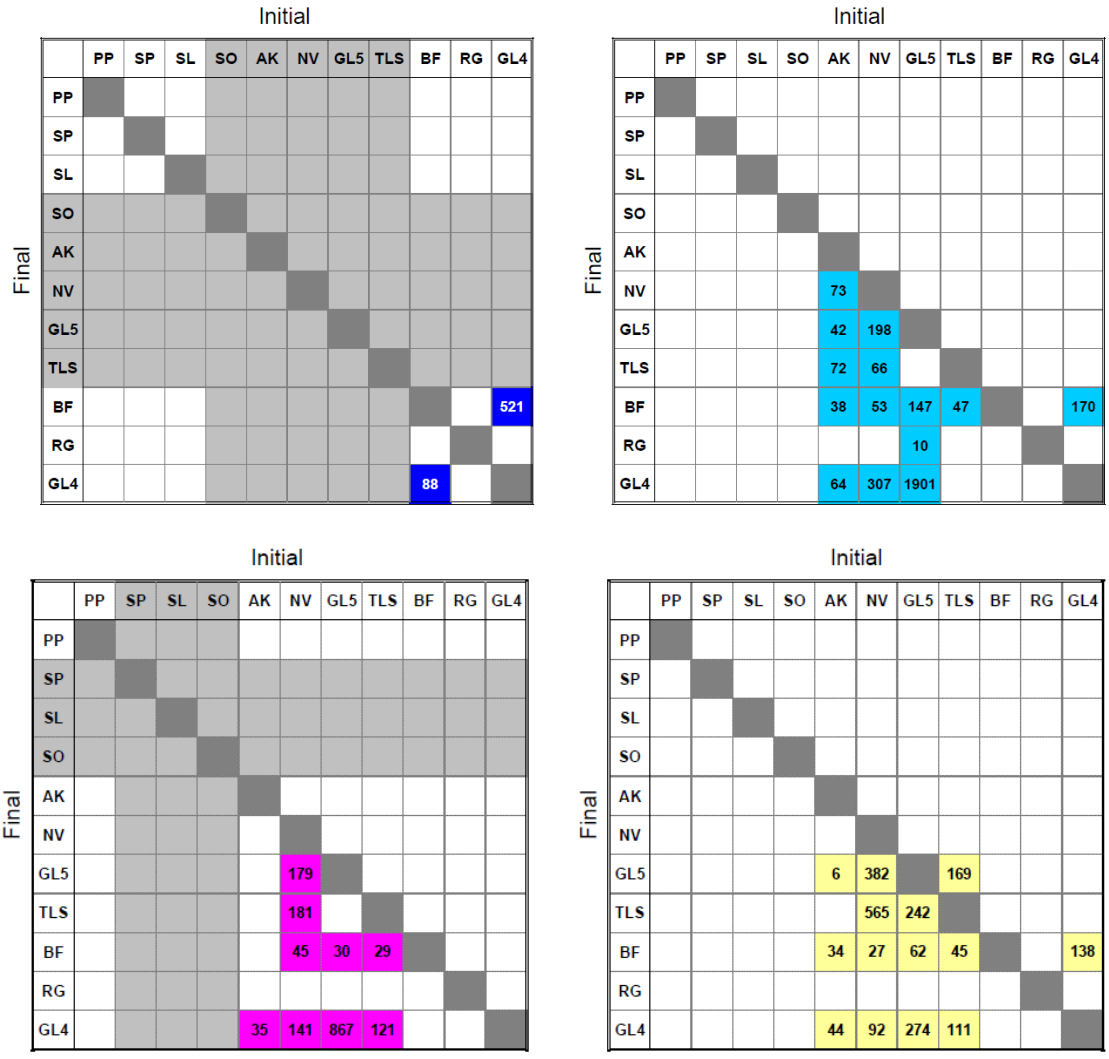

Figure 6: Result Grids for 1996 in GL4.
The above grids show the RPM results from Period A, Period B, Period C and the 1996 Average (clockwise from upper left). The light grey boxes in Periods A and C show where there were no samples collected at those end member locations for the given time period (during Period A this is because these locations were still frozen, in Period C because there was no longer any snowmelt). The numbers in the colored boxes show the number of possible combinations of geochemical weathering reactions to explain the difference between waters. The locations of the colored boxes are variable in each grid, showing the variability of geochemical connections over the snowmelt season.

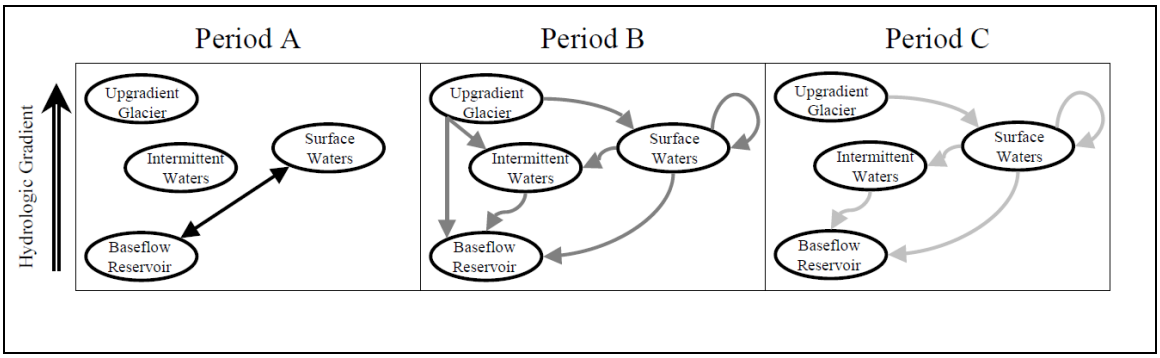

Figure 7: Conceptual model of flowpaths from RPM results.
Upgradient Glacier = AK, Surface Water = NV, GL5, GL4, Intermittent Waters = TLS, RG, Baseflow Reservoir = BF. Geochemical connections between each of these three categories each time period are shown with arrows. The most connections are seen during Period B, when there is the most water in the catchment. The difference between Period B and Period C is the lack of direct connection between the Upgradient Glacier and the Baseflow Reservoir. This geochemical connection is likely found because of the amount of water in the catchment during Period B, so that intermediate geochemical signatures were not seen in the path of these waters.

C. CHEMICAL DATA TABLES

Table A1: End member chemistry in mmol/L (Alkalinity in Eq/L) for Period A.

EM	pH	Si	Ca	Mg	Na	K	Alk	S(6)	Cl	N(+5)
PP	6.3526	0.0000	0.0727	0.0080	0.0314	0.0066	0.000	0.0296	0.0172	0.0016
SP	5.3733	0.0000	0.0038	0.0007	0.0017	0.0012	5.647	0.0027	0.0019	0.0053
SL	6.2400	0.0055	0.0864	0.0188	0.0377	0.0451	88.293	0.0451	0.0243	0.0473
EN4U	-	-	-	-	-	-	-	-	-	-
EN4M	-	-	-	-	-	-	-	-	-	-
EN4V	-	-	-	-	-	-	-	-	-	-
EN2M	-	-	-	-	-	-	-	-	-	-
EN2L	-	-	-	-	-	-	-	-	-	-
EN1U	-	-	-	-	-	-	-	-	-	-
EN1M	-	-	-	-	-	-	-	-	-	-
EN1L	-	-	-	-	-	-	-	-	-	-
SO	-	-	-	-	-	-	-	-	-	-
BF	6.3300	0.0384	0.0502	0.0102	0.0275	0.0103	79.100	0.0300	0.0099	0.0143
RG	6.4775	0.0446	0.0897	0.0206	0.0163	0.0239	51.800	0.0864	0.0042	0.0409
AK	-	-	-	-	-	-	-	-	-	-
GL4	6.4425	0.0302	0.0453	0.0097	0.0233	0.0114	68.122	0.0282	0.0081	0.0162

Table A2: End member chemistry in mmol/L (Alkalinity in Eq/L) for Period B.

EM	pH	Si	Ca	Mg	Na	K	Alk	S(6)	Cl	N(+5)
PP	5.3651	0.0000	0.0049	0.0008	0.0040	0.0006	0.000	0.0065	0.0030	0.0009
SP	5.3767	0.0015	0.0029	0.0011	0.0030	0.0026	7.410	0.0020	0.0039	0.0031
SL	6.1262	0.0038	0.0273	0.0079	0.0053	0.0123	45.309	0.0068	0.0057	0.0082
EN4U	5.9500	0.0059	0.0183	0.0049	0.0041	0.0074	24.320	0.0078	0.0032	0.0019
EN4M	6.3200	0.0210	0.0292	0.0054	0.0102	0.0050	53.570	0.0095	0.0020	0.0138
EN4V	6.0200	0.0102	0.0250	0.0043	0.0049	0.0043	30.020	0.0094	0.0032	0.0203
EN2M	5.9250	0.0099	0.0153	0.0034	0.0061	0.0026	20.410	0.0062	0.0053	0.0165
EN2L	5.9896	0.0164	0.0229	0.0054	0.0176	0.0031	26.245	0.0078	0.0035	0.0239
EN1U	-	-	-	-	-	-	-	-	-	-
EN1M	6.4586	0.0393	0.0395	0.0103	0.0185	0.0032	55.220	0.0102	0.0037	0.0355
EN1L	-	-	-	-	-	-	-	-	-	-
SO	6.2470	0.0307	0.0581	0.0200	0.0195	0.0609	44.218	0.0267	0.0558	0.0621
BF	6.3300	0.0384	0.0502	0.0102	0.0275	0.0103	79.100	0.0300	0.0099	0.0143
RG	6.6589	0.0542	0.1382	0.0305	0.0244	0.0338	73.600	0.1475	0.0050	0.0470
AK	5.2958	0.0065	0.0180	0.0038	0.0051	0.0033	-13.940	0.0122	0.0031	0.0293
GL4	6.2172	0.0213	0.0356	0.0083	0.0140	0.0095	33.645	0.0200	0.0045	0.0270

Table A3: End member chemistry in mmol/L (Alkalinity in Eq/L) for Period C.

EM	pH	Si	Ca	Mg	Na	K	Alk	S(6)	Cl	N(+5)
PP	5.0325	0.0000	0.0137	0.0019	0.0043	0.0016	0.000	0.0132	0.0040	0.0018
SP	-	-	-	-	-	-	-	-	-	-
SL	-	-	-	-	-	-	-	-	-	-
EN4U	6.1836	0.0199	0.0201	0.0031	0.0044	0.0035	32.740	0.0060	0.0014	0.0115
EN4M	6.6984	0.0351	0.0489	0.0085	0.0130	0.0061	74.208	0.0200	0.0018	0.0168
EN4V	6.7448	0.0385	0.0555	0.0099	0.0150	0.0062	73.620	0.0237	0.0023	0.0216
EN2M	6.1500	0.0178	0.0215	0.0045	0.0071	0.0033	15.620	0.0072	0.0022	0.0213
EN2L	6.2995	0.0383	0.0356	0.0078	0.0135	0.0038	31.530	0.0094	0.0035	0.0422
EN1U	5.7523	0.0066	0.0082	0.0020	0.0033	0.0012	9.793	0.0030	0.0015	0.0086
EN1M	6.5356	0.0311	0.0214	0.0059	0.0122	0.0026	43.922	0.0042	0.0029	0.0118
EN1L	6.5173	0.0332	0.0255	0.0055	0.0125	0.0019	51.174	0.0065	0.0016	0.0097
SO	-	-	-	-	-	-	-	-	-	-
BF	6.3300	0.0384	0.0502	0.0102	0.0275	0.0103	79.100	0.0300	0.0099	0.0143
RG	6.6800	0.0639	0.2740	0.0572	0.0329	0.0457	68.800	0.3088	0.0072	0.0574
AK	5.4704	0.0016	0.0060	0.0012	0.0032	0.0009	1.020	0.0035	0.0012	0.0079
GL4	6.4644	0.0213	0.0260	0.0054	0.0116	0.0036	37.578	0.0158	0.0020	0.0088

Table A4: End member chemistry in mmol/L (Alkalinity in Eq/L) averaged for 1996.

EM	pH	Si	Ca	Mg	Na	K	Alk	S(6)	Cl	N(+5)
PP	5.5561	0.0000	0.0304	0.0036	0.0132	0.0029	0.000	0.0164	0.0081	0.0014
SP	5.3750	0.0007	0.0033	0.0009	0.0023	0.0019	6.528	0.0023	0.0029	0.0045
SL	6.1828	0.0046	0.0568	0.0134	0.0215	0.0287	66.801	0.0259	0.0150	0.0229
EN4U	6.0657	0.0129	0.0192	0.0040	0.0042	0.0055	28.530	0.0069	0.0023	0.0141
EN4M	6.5065	0.0281	0.0391	0.0070	0.0116	0.0055	63.889	0.0147	0.0019	0.0162
EN4V	6.3721	0.0243	0.0402	0.0071	0.0099	0.0052	51.820	0.0165	0.0028	0.0208
EN2M	6.0365	0.0139	0.0184	0.0040	0.0066	0.0030	18.015	0.0067	0.0038	0.0181
EN2L	6.1426	0.0274	0.0293	0.0066	0.0155	0.0035	28.888	0.0086	0.0035	0.0330
EN1U	5.7523	0.0066	0.0082	0.0020	0.0033	0.0012	9.793	0.0030	0.0015	0.0086
EN1M	6.4970	0.0352	0.0305	0.0081	0.0154	0.0029	49.571	0.0072	0.0033	0.0197
EN1L	6.5173	0.0332	0.0255	0.0055	0.0125	0.0019	51.174	0.0065	0.0016	0.0097
SO	6.2470	0.0307	0.0581	0.0200	0.0195	0.0609	44.218	0.0267	0.0558	0.0621
BF	6.3300	0.0384	0.0502	0.0102	0.0275	0.0103	79.100	0.0300	0.0099	0.0143
RG	6.6048	0.0542	0.1673	0.0361	0.0245	0.0345	64.733	0.1809	0.0055	0.0471
AK	5.4325	0.0027	0.0086	0.0017	0.0036	0.0014	-2.186	0.0054	0.0017	0.0125
GL4	6.4331	0.0244	0.0329	0.0071	0.0153	0.0065	45.267	0.0201	0.0039	0.0139

D. MINERAL WEATHERING

The mineral weathering data from the PHREEQC results were summarized into Table 3. Each number in the table corresponds to a different phase, as shown below. The order of the numbers is based on the amount of each phase that has either dissolved or precipitated; the greatest amount of phase change is listed first. Not all phases present in the assemblage were dissolved or precipitated. Pyrite was not incorporated in any of the PHREEQC results.

The weathering reactions that were found to occur along the flowpaths were different for each end member combination. Most RPM flowpaths had many geochemical solutions with different combinations of weathering reactions to explain the compositional difference between catchment waters, as explained in Section 4.2. There is no explicit test to determine which of these reaction combinations was more accurate than another, although generally there were only minor changes between the solutions.

Box and whisker plots were made for each flowpath for each period to show the statistical spread of the RPM solutions for each combination of catchment waters (Figure 9). Flowpaths that ended in the same end member were compared, as well as overall weathering reactions for all flowpaths in the same period. All of the non-unique solutions found in PHREEQC were treated with equal weight, as there were no criteria by which to choose one solution over another. The physical amount of mineral weathering was not of particular concern, but rather the trend of either dissolution (positive flux) or precipitation (negative flux) of the mineral along the flowpath.

The direction of flux of CO_2 (positive indicating in-gassing, negative indicating out-gassing) was indicative of the completeness of weathering during the time period. In-gassing of CO_2 is indicative of weathering, out-gassing is indicative of lack of weathering. In-gassing of CO_2 will increase the alkalinity of the waters. The in-gassing and out-gassing of CO_2 for each flowpath is shown in Figure 10. This figure shows the same flowpath grid, but with "+" and "-" symbols indicative of the sign of the CO_2 flux. Positive values (+, in-gassing) for Period A, negative values (-, out-gassing) for Period B and both positive and negative values during Period C. Of note the only out-gassing flowpaths in Period C are the two flowpaths that also exist in Period B, perhaps indicating stages of weathering along these specific flowpaths.

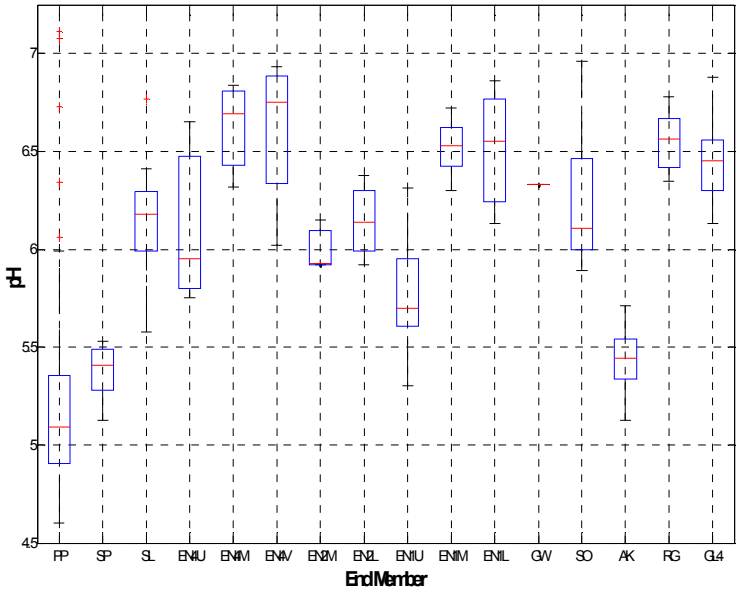

Figure 8: Box and whisker plot of pH values for catchment waters in GLV.
The arrows indicate potential flowpaths based on the buffering capacity of the geochemical reactions in the watershed. There are three groups of talus samples, EN4, EN2 and EN1. These three groups were sampled perpendicularly to the elevation contours. The talus samples from the highest elevations (U) have the lowest pH, which increases as the elevation decreases (M, L, V) along those groupings.

E. CO_2 RESULTS

Mineral weatheirng reactions are the main source of buffering capacity in these ecosystems. Alpine systems, due to their high altitude, geology, and biology have little buffering capacity. The ability of an alpine catchment to buffer acidic deposition is dependent on the mineral weathering and cation exchange processes.

Flowpaths during the different time periods showed a trend with regard to the CO_2 reactions. In-gassing of CO_2 means that there is CO_2 being added to the hydrochemical composition of the water, which increases the alkalinity. The increase of alkalinity results in incomplete mineral weathering reactions. The flux of CO_2 changes the alkalinity of the waters, which is associated with the ability of the catchment to buffer acidic atmospheric deposition [Williams and Tonnessen, 2000]

The results show that there is in-gassing of CO_2 during Period A, out-gassing during period B, and both in- and out- gassing during Period C. This change in weathering reactions between time periods means that alterations to these time periods will result in a change in the chemical reactions. Climate change drives earlier and shorter snowmelt seasons, which will create altered lengths of these time periods. These alterations could lead to altered flowpaths as well as altered chemical reactions along those flowpaths. A lack of initial in-gassing or a shortened period of out-gassing of CO_2 will result in an overall change in the weathering reactions, which in turn affect the buffering capacity of the catchment. The buffering capacity of the GL4 catchment to acidic atmospheric deposition was estimated based on the CO_2 in- and out-gassing in the

PHREEQC model. Overall CO_2 dissolution calculation for each weathering reaction for each period shows that the most buffering occurs after the snowpack has melted. The timing of this initial snowmelt, and the duration, therefore has a direct impact on the acidity of the waters in the catchment.

REFERENCES

Aleinikoff, J., E. DeWitt, J. C. Reed, Jr. and M. Walter, (1990), The Mount Evans batholith—an anomalous 1.4 Ga pluton in the Front Range, Colorado. *Geol. Soc. Am. Abstr. Prog., Rocky Mountain Sect*., *22,* 1.

Baron, J. S., and D. H. Campbell (1997), Nitrogen fluxes in a high elevation Rocky Mountain basin, *Hydrological Processes*, *11*, 783-799.

Bassett, R. L., (1997), Chemical modeling on the bare rock or forested watershed scale. *Hydrological Processes, 11*, 695-717.

Brooks, P. D., and M. W. Williams (1999), Snowpack controls on nitrogen cycling and export in seasonally snow-covered catchments, *Hydrological Processes*, *13*, 2177-2190.

Brooks, P. D., et al. (1996), Microbial activity under alpine snowpacks, Niwot Ridge, Colorado, *Biogeochemistry*, *32*, 93-113.

Brooks, P. D., et al. (1998), Inorganic nitrogen and microbial biomass dynamics before and during spring snowmelt, *Biogeochemistry*, *43*, 1-15.

Brown, A. D. (1995), Rock, Water, Soil Interactions at Sierra Nevada High Elevations, *in Atmospheric Acidity Protection Program Assessment Workshop, edited by W. J. Mautz, California Air Resources Board, Sacramento, CA*, 381-393.

Caine, N. (1995), Temporal trends in the quality of streamwater in an Alpine environment: Green Lakes valley, Colorado Front Range, USA, *Geografiska Annaler Series A-Physical Geography*, *77A*, 207-220.

Caine, N., E.M. Thurman (1990), Temporal and spatial variations in the solute content of an alpine stream, Colorado Front Range, *Geomorphology, 4,* 55-72.

Campbell, D. H., D. W. Clow, G. P. Ingersoll, M. A. Mast, N. E. Spahr, J. T. Turk, (1995), Processes controlling the chemistry of two snowmelt-dominated streams in the Rocky Mountains, *Water Resources Research, 31*, 2811-2821.

Carroll, S.S. and N. Cressie (1996), A comparison of geostatistical methodologies used to estimate snow water equivalent, *Journal of the American Water Resources Association, 32,* 267.

Christopherson N., R.P. Hooper (1992), Multivariate analysis of stream water chemical data: the use of principal components analysis for the end-member mixing problem. *Water Resources Research, 28*, 99–107.

Christopherson N., C. Neal, R.P. Hooper, R.D. Vogt, S.C.S. Andersen. (1990). Modelling streamwater chemistry as a mixture of soil water end- members—a step towards second-generation acidification models. *Journal of Hydrology, 116,*307–320

Cline, D. W., et al. (1998), Estimating the spatial distribution of snow in mountain basins using remote sensing and energy balance modeling, *Water Resources Research*, *34*, 1275-1285.

Clow, D. W., et al. (1997), Strontium 87 strontium 86 as a tracer of mineral weathering reactions and calcium sources in an alpine/subalpine watershed, Loch Vale, Colorado, *Water Resources Research*, *33*, 1335-1351.

Clow, D.W., L. Schrott, R. Webb, D.H. Campbell, A. Torizzo, M. Dornblaser (2003), Ground water occurance and contributions to streamflow in an alpine catchment, Colorado Front Range, *Groundwater*, *41*, 937-950.

Doesken and Judson, (1997) *The Snow Booklet: A Guide to the Science, Climatology, and Measurement of Snow in the United States*, Department of Atmospheric Science, Colorado State University, Colorado, USA.

Drever, J.I. (1988), *The Geochemistry of Natural Waters*, Prentice Hall, Englewood Cliffs, N.J., USA.

Drever and Clow (1995), Weathering rates in catchments, *Reviews in Mineralogy and Geochemistry, 31*, 463-483.

Fassnacht, S.R., K.A. Dressler, R.C. Bales, (2003), Snow water equivalent interpolation for the Colorado River Basin from snow telemetry (SNOTEL) data, *Water Resources Research, 39*, 1208.

Garrels, R.M. and F.T. MacKenzie (1971), *Evolution of sedimentary rocks*, Norton, New York, New York, USA.

Hooper, R. P., and N. Christophersen (1992), Predicting Episodic Stream Acidification In The Southeastern United-States - Combining A Long-Term Acidification Model And The End-Member Mixing Concept, *Water Resources Research*, *28*, 1983-1990.

Liator, M.I., (1987) Aluminum chemistry: Fractionation, speciation, an mineral equlibria of soil interstitial waters of an alpine watershed, Front Range, Colorado. *Geochemica et Cosmochimica Acta, 51*, 1285-1295.

Liu, F. J., et al. (2004), Source waters and flow paths in an alpine catchment, Colorado Front Range, United States, *Water Resources Research*, *40*.

Mast, M.A., and J.I. Drever (1990), Chemical weathering in the Loch Vale Wateshed, Rocky Mountain National Park, Colorado, *Water Resources Research, 26*, 2971-2978.

Melack, J.M. and J.L. Stoddard (1991), "Sierra Nevada", in *Acidic Deposition and Aquatic Ecosystems: Regional Case Studies*, D.F. Charles (ed.), Springer-Verlag, New York, NY, 503-530.

Meixner, T., and R. C. Bales (2003), Hydrochemical modeling of coupled C and N cycling in high-elevation catchments: Importance of snow cover, *Biogeochemistry*, *62*, 289-308.

Meixner, T., et al. (2000), Stream chemistry modeling of two watersheds in the Front Range, Colorado, *Water Resources Research*, *36*, 77-87.

Molotch, N. P., M.T. Colee, R.C.Bales, J. Dozier (2005), Estimating the spatial distribution of snow water equivalent in an alpine basin using binary regression tree models: the impact of digital elevation data and independent variable selection, *Hydrological Processes*, *19*, 1459-1479.

Molotch, N., T. Meixner, M.W. Williams (in review), Estimating stream chemistry during the snowmelt pulse using a spatially distributed, coupled snowmelt and hydrochemical modeling approach, *Water Resources Research*.

Neal, C. (2001), Alkalinity measurements within natural water: towards a standarised approach, *The Science of the Total Environment, 265*, 99-113.

Nesse, W.D. (2000), *Introduction to Mineralogy*, Oxford University Press, Inc., New York, NY, USA.

Parkhurst, D.L. and C.A.J. Appelo (1991), User's guide to PHREEQC (Version 2)—a computer program for speciation, batch-reaction, one-dimensional transport, and inverse geochemical calculations, *Water-Resources Investigations Report*, 99-4259.

Parkhurst, D.L. (1997), Geochemical mole-balance modeling with uncertain data, *Water Resources Research, 33*, 1957-1970.

Plummer, L.N., D. L. Parkhurst, D. C. Thorstenson (1983), Development of reaction models for ground-water systems, *Geochemica et Cosmochimica Acta, 47,* 665-686.

Platts-Mills and Williams (2005), Selectivity of mineral weathering, personal communication.

Sickman, J. O., et al. (2001), Nitrogen mass balances and abiotic controls on N retention and yield in high-elevation catchments of the Sierra Nevada, California, United States, *Water Resources Research*, *37*, 1445-1461.

Stewart, I. T., D. R. Cayan, M. D. Dettinger (2004), Changes in snowmelt runoff timing in Western North America under a 'buisness as usual' climate change scenario, *Climatic Change*, *62*, 217-232.

Sueker, J. K., et al. (2000), Determination of hydrologic pathways during snowmelt for alpine/subalpine basins, Rocky Mountain National Park, Colorado, *Water Resources Research*, *36*, 63-75.

Wolford, R. A., R. C. Bales, and S. Sorooshian (1992), Integrated hydrochemical modeling of an alpine watershed: Sierra Nevada, California, dissertation.

Wolford, R. A., R. C. Bales, and S. Sorooshian (1996), Development of a hydrochemical model for seasonally snow-covered alpine watersheds: Application to Emerald Lake watershed, Sierra Nevada, California, *Water Resources Research*, *32*, 1061-1074.

Williams, M. W., D. Cline, M. Hartman, and T. Bardsley (1999), Data for snowmelt model development, calibration, and verification at an alpine site, Colorado Front Range, *Water Resources Research*, *35*, 3205-3209.

Williams, M.W., M. Losleben, N. Caine, and D. Greenland (1996) Changes in climate and hyrochemical responses in a high-elevation catchment, Rocky Mountains, *Liminol. Oceanogr., 41,* 939-946.

Williams, M.W. and J. M. Melack (1991a), Precipitation chemistry in and ionic loading to an alpine basin, Sierra Nevada, *Water Resour. Res., 27*, 1563-1574.

Williams, M.W. and J.M. Melack (1991b), Solute chemistry of snowmelt and runoff in an alpine basin, Sierra Nevada, *Water Resour. Res., 27*, 1575-1588.

Williams, M.W. and K.A. Tonnessen (2000), Critical loads for inorganic nitrogen deposition in the Colorado Front Range, USA, *Ecological Applications,10*, 1648–1665.